6.0 STUDY 4 - EVALUATE EXISTING RADIATION FIELDS

J. M. Aldrich, D. L. Haggard, G. W. R. Endres, and J. J. Fix

FOREWORD

Knowledge of the spectrum of energies for beta, gamma, and neutron radiation experienced in the field is crucial to the proper interpretation of personnel dose. Calibration sources and techniques are determined on the basis of their relationship to field exposures. This study describes the measurement techniques used, particularly for neutrons, and, in appendices, the data obtained for several locations at Hanford during FY-1981.

SUMMARY

During FY-1980, field measurements were taken at the following locations:

		Measurements[a]
308 Building	Fuel Storage Pit Area	MS, TEPC, RASCAL, HMPD
	Plutonium Storage Vault	MS, TEPC, RASCAL
	Fuel Pin Storage Box Area	MS, TEPC, RASCAL
	Bare Fuel Subassembly	MS, TEPC, RASCAL, HMPD
	Room Background	Gamma
	Grinder Hood Bottom	Gamma
	Pellet Pressing Station	Gamma
327 Building	Background - A Cell	Gamma
	Background - G Cell	Gamma
2425-200W	Evaporator Building - NE Corner	Gamma
200 W-Diversion Boxes	241-TX-302-C Catch Tank	Gamma
	K2U	Gamma
	Rigging Crew	Beta
B-Plant (225 Building)	A Cell	Gamma
	Between B-C Cells	Gamma
	Between D-E Cells	Gamma
	F Cell	Gamma
	Room Background	Gamma
271B	Pipe Gallery - Cell 9	Beta
234-5	Glovebox H-9A	MS, TEPC, SNOOPY, HMPD
	Glovebox HC-9B	MS, TEPC, SNOOPY, HMPD
2736-Z	Six locations in building	MS, TEPC, SNOOPY, HMPD

(a) MS - multisphere system, TEPC - tissue equivalent proportional counter, HMPD - Hanford multipurpose personnel dosimeter.

Generally neutron dose equivalent rate measurements with the multisphere system, TEPC, and SNOOPY were consistent with each other. The RASCAL indicated dose equivalent rates about a factor of two higher. Dose equivalent rates were generally very low resulting in uncertainties in the small integral doses recorded by the Hanford dosimeters. Average neutron energies for different locations were observed from about 150 keV (hallway in 2736-Z Building) to 1.5 MeV (midpoint of the bare fuel subsassembly in 308 Building). Gamma measurements snowed ^{137}Cs to be the predominate nuclide at B-Plant and at the 200 West Diversion box. At the 308 Building, ^{241}Am was the predominant gamma emitting nuclide observed. At 327, ^{137}Cs, ^{54}Mn, and ^{60}Co were observed. Beta measurements obtained using a modified Hanford dosimeter worn by a rigging crew in the 200 Area showed generally penetrating radiation only. Beta measurements collected in the 271B pipe gallery and a diversion box showed a low energy beta component.

An observation of significance for proper field use of the personnel dosimeter is the reduced response of the dosimeter to neutrons incident to the side of the dosimeter or to the back of the phantom (or person) relative to an instrument response which has an effective full 360° response. Whenever a significant neutron flux is incident on a person wearing a dosimeter from any direction other than in front, the dosimeter will underresponse. Countering this effect is the overresponse of the dosimeter for neutrons less than the calibration neutron spectrum (mean energy about 1 MeV).

INTRODUCTION

Selected techniques were used to obtain neutron, photon, and beta energy spectra data at several Hanford locations. Four neutron energy spectra and dose measurement methods were used:

1. Multisphere spectrometer system
2. Tissue equivalent proportional counter (TEPC)
3. RASCAL[(a)] (9" to 3" sphere ratios)
4. Helium-3 neutron spectrometer.

(a) Portable neutron rem counter manufactured by Eberline, Santa Fe, New Mexico.

Gamma spectroscopy was done using standard techniques. A specially designed TLD dosimeter was used to obtain beta spectrum measurements.

The design and use of each of these instruments is described in the body of this report. Data collected and analyzed for each of the Hanford locations are included in appendices for each location.

MATERIALS AND METHODS

Measurement systems employed during this study were selected to characterize the energy spectrum of the predominate radiation type(s) at each location. Complementary neutron instrumentation was used to better characterize the neutron radiation at several locations. Gamma fields were characterized according to predominant radionuclides. An approximation of the beta field energy was obtained using a multifiltered TLD dosimeter. There is no convenient field instrument to characterize beta energies.

Multisphere Spectrometer System

The multisphere neutron system (Awschalom 1966) and specific instrument settings used in this work are shown in the block diagram in Figure 6.1. Multispheres are the best available commercial system for measuring intermediate neutron energy spectra (1 keV to 1 MeV) (Griffith and Fisher 1976) and are also capable of detecting neutrons in the thermal to 1 keV energy range. When the multisphere system is used with a spectrum unfolding code such as

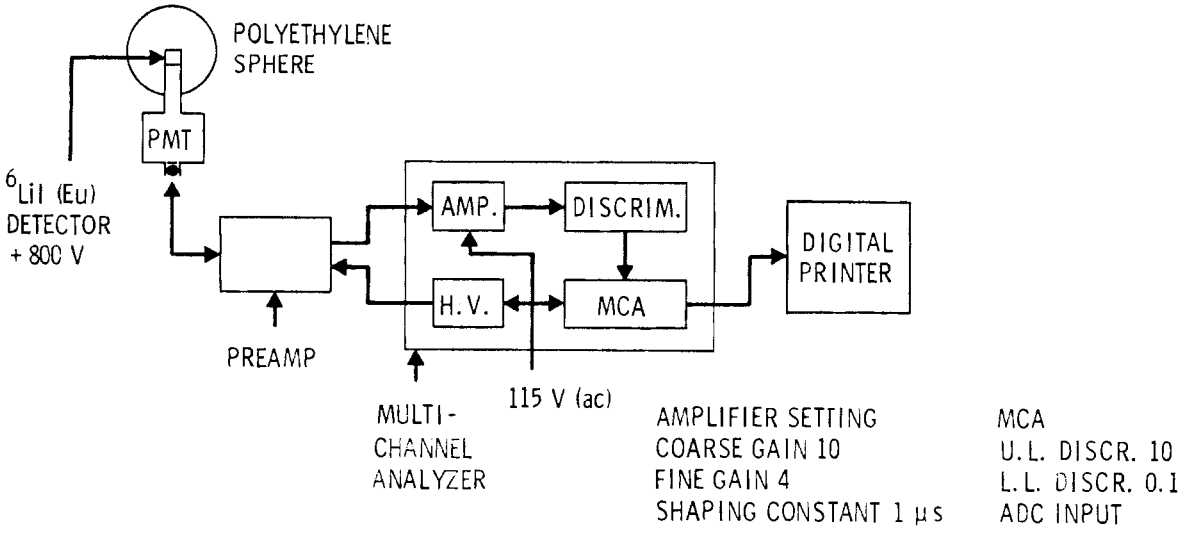

FIGURE 6.1. Block Diagram of the Multisphere System

LOUHI (Routti and Sandberg 1978), the average neutron energy, dose equivalent rate, total flux, kerma, and graphical plots of differential flux versus energy, flux per unit lethargy versus energy, and flux versus energy can be obtained. The detector is a cylindrical $^{6}LiI(Eu)$ scintillation crystal, 1.27 cm in diameter by 1.27 cm long, optically coupled to a 20.32 cm light pipe which in turn is optically coupled to a photomultipler tube (PMT). The detector and its integral components are hermetically sealed in an aluminum tube with walls 0.16 cm thick. The PMT is surrounded by a brass sleeve for protection and support for cable connectors. A single cable carries both the high voltage and output signals, connecting the detector to a preamplifier which decouples the signals and feeds them into the multichannel analyzer (MCA). This analyzer has three built-in systems as intergral parts: amplifer, high voltage power supply, and discriminators. The unanalyzed data is directly obtained from the MCA and fed to a digital printer for hard copy.

The neutron detection mechanism exhibited by the $^{6}LiI(Eu)$ crystal is the $^{6}Li(n,\alpha)^{3}H$ reaction for thermal neutrons. This reaction is exoergic and deposits an equivalent electron energy of 4.8 MeV in the scintillator, producing a distinct peak in the pulse height spectrum shown on the MCA. There are no other competing peaks in the spectrum. An exponential background continuum is subtracted from the full width peak area.

Unanalyzed data for the neutron energy spectrum are obtained by taking counts with the scintillation crystal unshielded (bare), with the crystal in a cadmium shell (0.051 cm thick), and with the crystal moderated by spheres of high density polyethylene (7.6, 12.7, 20.3, 25.5, and 30.5 cm in diameter). The fast neutron response of this sytem increases with sphere size because the larger polyethylene spheres remove low energy neutrons by scattering and moderate the fast neutrons to lower energies where they are then detected with a greater probability by the $^{6}LiI(Eu)$ scintillator. Cadmium shells placed around the 7.6 and 12.7 spheres suppress response to external thermal neutron fields which improves the detectability of the system to moderated fast neutrons above cadmium cutoff (0.4 eV) (Hankins and Griffith 1979).

Using the responses from the seven detector configurations (bare, cadmium covered, 7.6, 12.7, 20.3, 25.5, and 30.5 cm moderators) the spectrum is unfolded with the aid of the LOUHI computer code. LOUHI is a FORTRAN program written to solve Fredholm integral equations of the first kind by using a generalized least-squares procedure with non-negative solutions. With LOUHI, the spectral solution is not dependent on the choice of initial approximation. Through prior knowledge of the flux in a particular part of the spectrum, the solution in the appropriate energy bin can be "tied" to that point (Hajnal 1979). The energy bin referred to is the 26^{th} bin or upper limit of the energy range over which the spectrum is to be calculated. This becomes the "tied" point and is based on the response of the 12.7 cm sphere. For this study, this feature is used to place the high energy bin at a realistic value which reflects the general lack of source neutrons above 14 MeV (Hankins and Griffith 1979; Hajnal 1979).

Neutron energy response functions calculated by Sanna (1973) are used as input for the unfolding process. Sanna's calculations are based on one dimensional spherical geometries and were verified empirically in the energy range 100 keV to 20 MeV (Griffith and Fisher 1976). To make the sphere responses equal to Sanna's calculations in this energy range, density corrections for the spheres are performed by the LOUHI code.

Essentially, the basic equations of LOUHI solve for neutron flux, absorbed dose, average neutron energy, and dose equivalent rate. LOUHI uses equation (1) to determine neutron flux in the j^{th} energy band, ϕ_j:

$$A_i = \sum_{j=1}^{26} R_{ij}\, \phi_j \qquad (1)$$

where:

A_i = the count rate with the i^{th} detector configuration, and is obtained by integrating under the peak using a log background subtraction continuum and dividing that value by the count time for each individual detector configuration, and

R_{ij} = the response function of the i^{th} detector in the j^{th} energy band calculated by Sanna (1973), and is directly available from his tabulations.

The average neutron energy calculation incorporates a weighting function shown in equation (2):

$$Eav = \sum_{j=1}^{n} w_j \cdot E_j \cdot F_j \cdot F_s^{-1} \qquad (2)$$

where: Eav = average neutron energy
j = energy band (1-26)
n = total number of energy bands (26)
w_j = weighting function of j^{th} energy band
E_j = energy value at the j^{th} point, in MeV
F_j = the solution at point j
F_s = total flux

The dose equivalent rate equation uses a weighting function and a precalculated neutron flux to dose equivalent conversion ratio as shown in equation (3):

$$DS = \sum_{j=1}^{n} w_j \cdot d_j \cdot F_j \qquad (3)$$

where: DS = dose equivalent rate
n, j, w_j, and F_j = are the same as equation (2)
d_j = neutron flux to dose equivalent conversion factor.

Flux-to-dose equivalent conversion factors are compiled as a subroutine in the LOUHI program and have been taken directly from tables in ICRP 21 (1971). Absorbed dose calculations are performed in a subroutine called element 57 dose rate, developed at Oak Ridge National Laboratory. This model is used to estimate the dose in various regions of a homogenous anthropomorphic phantom, which was taken as a right cylinder with a radius of 15 cm and a height of 60 cm. Composition of the phantom was assumed to be H, C, N, and O in the proportions of standard man. The cylindrical volume was divided into 150 numbered volume elements and the average dose per neutron flux in the incident beam was computed for each volume element. The neutron beam was assumed to be broad enough to irradiate the whole phantom and to be monoenergetic and monodirectional with velocity vector parallel to the base of the

cylinder (Auxier, Snyder, and Jones 1968). The maximum dose rate, in this scheme, is to Element 57. Thus, the Element 57 dose rate is considered to be the best estimate for depth dose rate at the energy levels measured in reactors.

Quality factors are not directly calculated by the LOUHI unfolding code but can be easily determined by dividing the dose equivalent rate by the Element 57 absorbed dose rate. A QF value determined by this method will not be the same as the QF value calculated by the TEPC. The significance of this point will become more apparent as it is shown that both systems derive dose equivalent rates and QF's from different methodologies. Further detailed discussion of the LOUHI program is readily available in the literature (Awschalom 1966; Routti and Sandberg 1978; Bramblett, Ewing and Bonner 1960).

There are two sphere sizes sometimes associated with the multisphere which were not used in this study; they are the 5.08 cm and 45.7 cm diameter spheres. The smaller of the two, the 5.08 cm sphere, produces a response very nearly equal to that of the cadmium shielded detector. Because of the size of the hole bored into the sphere, to accommodate the detector, it is not known whether the response is valid in this system. Therefore, a well-defined cadmium cutoff point of 0.4 eV is established as the next to lowest energy band (the response of the bare detector being the lowest). The larger sphere 45.7 cm, would normally be used to provide a response in the energy range of >3 MeV. Since the responses of the 30.5 cm diameter sphere and the 45.7m diameter sphere are nearly identical for the spectra of concern, the larger sphere was not used.

A typical multisphere data table generated by the LOUHI code shows the calculated fluxes, energies, and integral dose equivalents over the 26 points with the final results compiled at the bottom of the table (see Table 6.1). Two of the plots developed from the data table are a differential spectrum versus energy and flux per unit lethargy versus energy spectrum.

Table 6.1. Typical Set of Multisphere Data

	E(I) MeV	DIFFERENTIAL FLUX (n/cm^2 - MeV - sec)	INTEGRAL FLUX	INTEGRAL DOSE EQUIVALENT	ENERGY BAND (MeV)	FLUX (n/cm^2 - sec)
1	2.07E-07	3.77E+08	1.00E+00	1.00E+00	3.89E-07	1.47E+02
2	5.32E-07	5.16E+07	8.03E-01	9.28E-01	2.69E-07	1.39E+01
3	9.93E-07	8.52E+06	7.85E-01	9.20E-01	7.63E-07	6.50E+00
4	2.10E-06	1.83E+06	7.76E-01	9.17E-01	1.61E-06	2.95E+00
5	4.45E-06	5.14E+05	7.72E-01	9.15E-01	3.42E-06	1.76E+00
6	9.42E-01	1.88E+05	7.70E-01	9.15E-01	7.22E-06	1.36E+00
7	2.00E-05	8.73E+04	7.68E-01	9.14E-01	1.53E-05	1.34E+00
8	4.22E-05	4.99E+04	7.66E-01	9.13E-01	3.23E-05	1.61E+00
9	8.94E-05	3.40E+04	7.64E-01	9.12E-01	6.89E-05	2.34E+00
10	1.89E-04	2.65E+04	7.61E-01	9.11E-01	1.45E-04	3.84E+00
11	4.04E-04	2.27E+04	7.55E-01	9.10E-01	3.18E-04	7.22E+00
12	8.55E-04	2.03E+04	7.46E-01	9.06E-01	6.40E-04	1.30E+01
13	1.80E-03	1.82E+04	7.28E-01	9.01E-01	1.38E-03	2.51E+01
14	3.80E-03	1.54E+04	6.95E-01	8.90E-01	2.91E-03	4.48E+01
15	8.05E-03	1.17E+04	6.34E-01	8.70E-01	6.20E-03	7.25E+01
16	1.70E-02	7.64E+03	5.37E-01	8.40E-01	1.30E-02	9.93E+01
17	3.61E-02	4.04E+03	4.03E-01	7.75E-01	2.77E-02	1.12E+02
18	7.64E-02	1.65E+03	2.53E-01	6.48E-01	5.86E-02	9.67E+01
19	1.58E-01	5.00E+02	1.23E-01	4.54E-01	1.13E-01	5.56E+01
20	3.18E-01	1.10E+02	4.74E-02	2.60E-01	2.27E-01	2.50E+01
21	6.40E-01	1.75E+01	1.39E-02	1.15E-01	4.56E-01	7.98E+00
22	1.29E+00	2.12E+00	3.22E-03	3.61E-02	9.20E-01	1.95E+00
23	2.59E+00	2.05E-01	6.06E-04	7.17E-03	1.85E+00	3.79E-01
24	5.22E+00	1.68E-02	9.76E-05	1.22E-03	3.73E+00	6.27E-02
25	1.05E+01	1.23E-03	1.37E-05	1.79E-04	7.50E+00	9.23E-03
26	1.96E+01	8.56E-05	1.25E-06	1.72E-05	1.09E+01	9.33E-04

TOTAL FLUX = 7.4477E+02 NEUTRONS / SQ. Cm. / SEC.
DOSE EQUIVALENT RATE = 8.5643E+00 Mrem / HOUR
ELEMENT 57 DOSE RATE = 1.6681E-03 RADS / HOUR
AVERAGE ENERGY = 5.3385E-02 MeV

Tissue Equivalent Proportional Counter (TEPC)

The tissue equivalent proportional counter (TEPC) system measures the absorbed dose and the TEPC computer code calculates the dose distribution as a function of event size and LET. The TEPC computer code also calculates a quality factor by using the Rossi analysis (Rossi 1968) and several approximations derived by Brackenbush, Endres and Faust (date). A block diagram of the TEPC system and instrumentation settings is shown in Figure 6.2 The electronic system components include detector, preamplifer, amplifier, and high voltage power supply. The multichannel analyzer (MCA) used with the TEPC has a log display. This log display greatly assists in the preliminary interpretation of the unanalyzed data. Figure 6.3 shows the multisphere, TEPC, and associated electronic systems.

The TEPC is a hollow sphere of tissue equivalent plastic (Shonka A150 muscle equivalent plastic with the walls 3.2 mm thick) filled with methane-based tissue equivalent gas. Details of plastic and gas composition and methods of construction can be found in ICRU Report 26 (1977). This form of TEPC, called a Rossi counter, has a helical grid around the central anode wire. The helical grid establishes uniform lines of force along the entire length of the anode. This produces the needed uniformity in gas amplification at all points along the anode for proper pulse height analysis. The plastic sphere is contained inside a metal pressure vessel with a valve for admitting tissue equivalent gas. The gas pressure is maintained at a low pressure of 5.6 mm Hg absolute so that charged particles crossing the cavity lose only a small amount of energy as they transverse the counter. Energy deposited in the cavity is then equal to the linear energy transfer of the particle times the path length. At these low pressures the gas-filled cavity has the same mass stopping power as a sphere of tissue (ρ = 1 gm/cm^3) with a diameter of about one micrometer and is said to have an "equivalent diameter" of one micrometer.

The TEPC becomes self-calibrating when the proton drop point is identified. A proton drop point corresponds to a slow proton recoil having the highest linear energy transfer or transversing the diameter of the spherical cavity and is independent of the initial energy of the neutron producing the

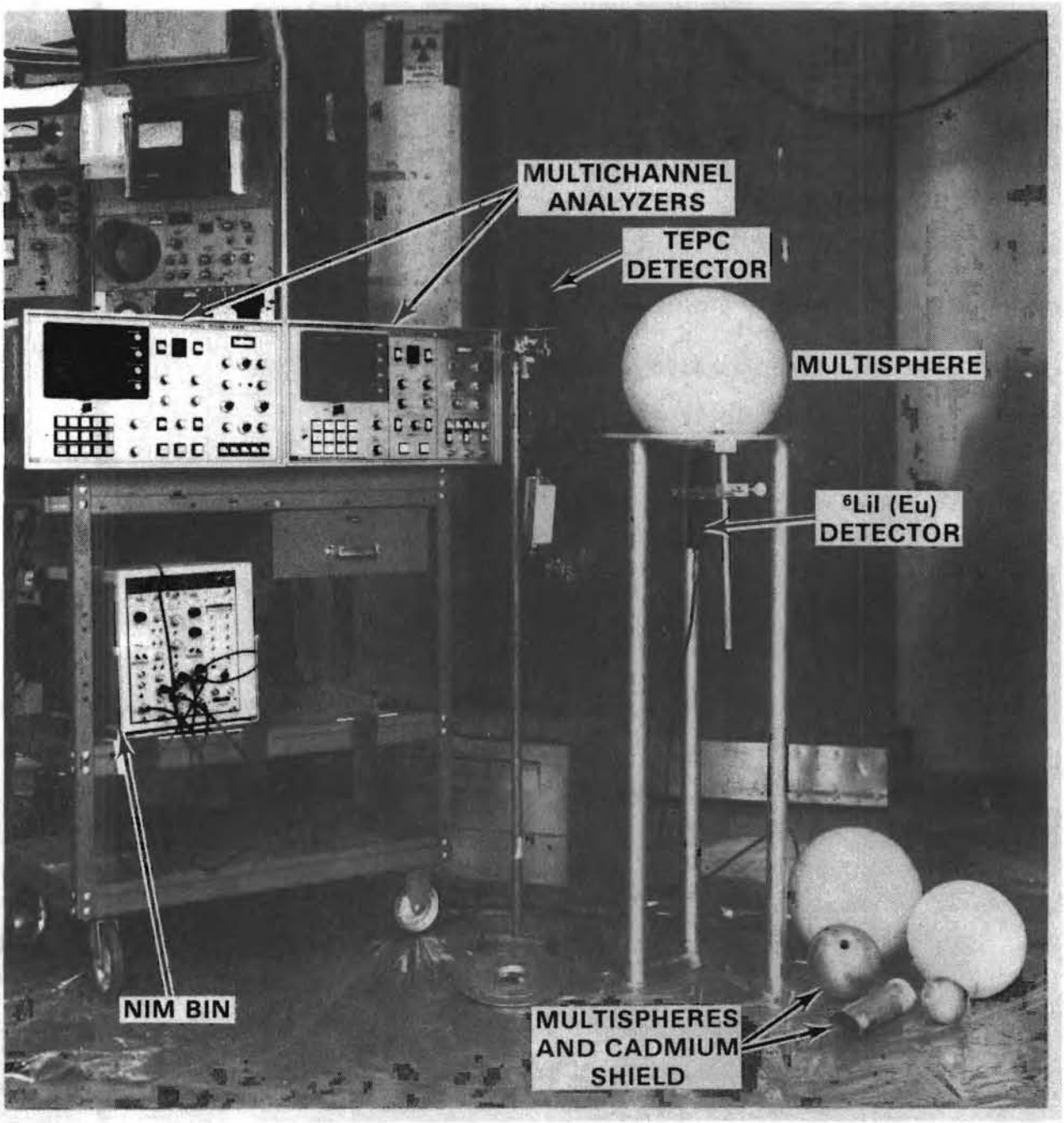

FIGURE 6.2. Multisphere Spectrometer and TEPC Systems

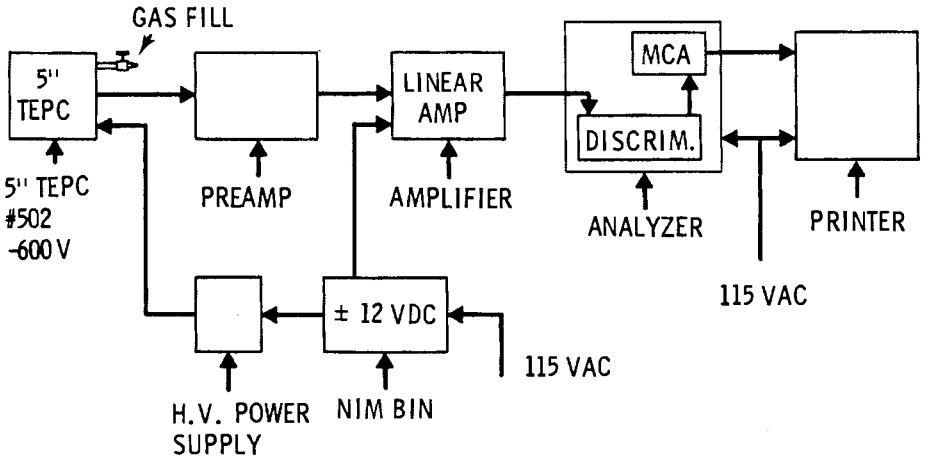

LINEAR AMP SETTINGS	MCA
COARSE GAIN 10	LOG SCALE
FINE GAIN 6.0	ZERO SETTING 2.65
SHAPING CONSTANT 1μ sec	U.L. DISCR. 10
	L.L. DISCR. 0
BASE LINE RESTORER BLR	
1) ASYMMETRY - x1	ACQ (ACQUIRE MODE)
2) RATE - HIGH	DIRECT
3) GATE - IN	OFF
UNIPOLAR OUTPUT - POSITIVE	INPUT IS IN DIRECT

FIGURE 6.3. Block Diagram of TEPC System

event. According to the data of Glass and Samsky (1967), this point occurs at about 100 keV/μm and is a slowly varying function of tissue-equivalent gas pressure.

Multiplying the number of events of a given size by the energy of the event gives the absorbed energy distribution in the TE gas, which is a direct measure of absorbed dose. Following the nomenclature in ICRU 26 (1977), this is stated in equation (4):

$$D = 1.602 \times 10^{-8} \sum_{h_1}^{h_2} k \cdot h \cdot N(h) \cdot V^{-1} \cdot \rho^{-1} \qquad (4)$$

where:

D = absorbed dose (rad)

h = the measured pulse height expressed as channel number

N(h) = the number of pulses accumulated in channel h, h_1, and h_2 are the limits in pulse height between which the absorbed dose is to be determined

ρ = the gas density, in gm cm^{-3}

V = the sensitive volume of the cavity in cm^3

k = the calibration relating energy to channel number, which was determined from the proton drop point (keV/channel number).

For calculational purposes: h_1, the lower limit of event size, is defined as the minimum between photon and neutron induced events which occurs at an event size of about 15 keV/μm, and h_2 is the upper limit of the event size spectrum. The summation over N(h) between h_1 and h_2, as shown in equation (4), is the total energy absorbed in the gas cavity due to high LET events. The measured neutron dose, D, is the energy absorbed in the gas cavity divided by the mass of TE gas inside the sphere.

The TEPC event spectrum (Figure 6.4) shows the number of events per channel, commonly referred to as the energy deposited per channel or event size spectrum. Also shown in Figure 6.4 are the three parameters needed to analyze TEPC data: h_1, the lower limit; h_2, the upper limit; and the proton drop point.

TEPC DOSE EQUIVALENT

The only general method that has been developed for the measurement of the distribution of dose in LET is based on an analysis of the frequency distribution of the event size due to individual particles in a spherical volume of tissue, that is, the N(y) distribution. Actual distributions are different from those derived with the assumptions that energy loss is continuous and that particles travel in straight lines and have a range that is infinitely long compared with cavity diameter. These same assumptions are made in the derivation of the LET spectrum from event-size spectrum; it is evident that error is introduced. Also X-rays, electrons, $H(n,\gamma)D$ reactions, and positrons

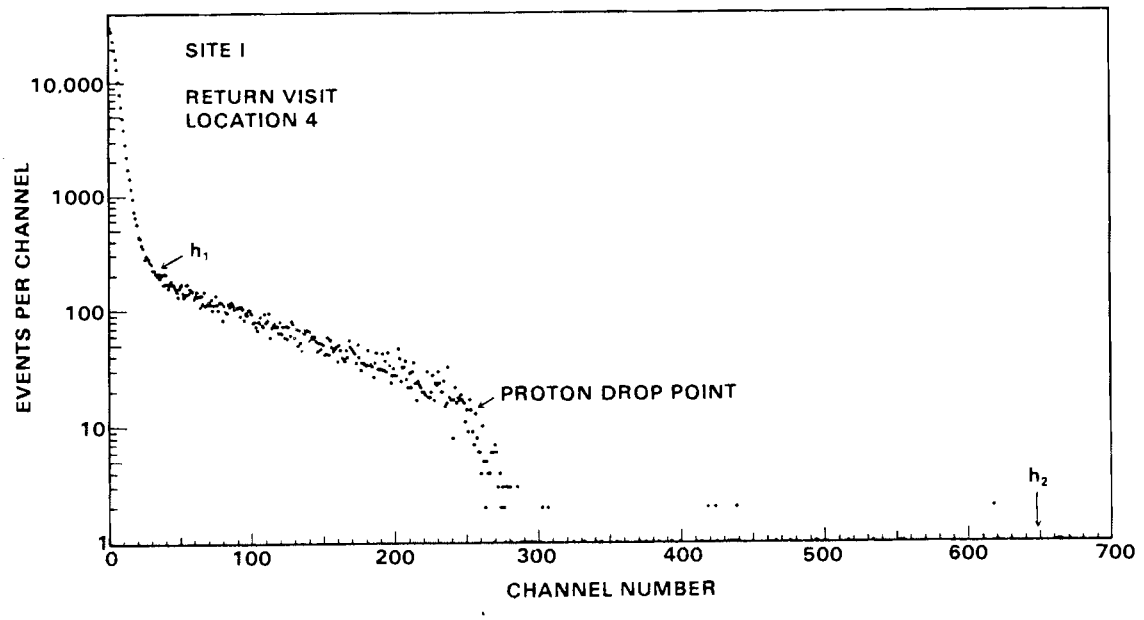

FIGURE 6.4. TEPC Event Size Spectrum

are assigned a QF of 1, which does not add significantly (<0.1) to the calculated dose equivalent. Most of these events are below the lower limit (h_1) used in spectral analysis. However, discrepancies between experimental and theoretical spectra are usually sufficiently small so as to be acceptable for purposes of radiation protection. It has been Rossi's development of this technique, using the above assumptions, that has led to a determination of dose equivalent rates by calculating absorbed dose as a function of LET and by using QF as a function of LET described in ICRU 20 and ICRU 26 (1977; 1976).

H. H. Rossi devised a relatively simple model to determine the absorbed dose distribution as a function of linear energy transfer (Rossi 1968). In ICRU 26, QFs are defined in terms of LET which makes it possible to determine dose equivalent rates and QFs from a single TEPC measurement. The Rossi model employs a spherical counter with neutron recoils arising within the walls and assumes the recoil have a constant, uniform energy loss along a straight line and completely cross the cavity. Under these assumptions, the absorbed dose distribution within the cavity as a function of LET, D(L) can be calculated by equation (5) (Rossi 1968).

$$D(L) = \frac{k}{r^2} \left[y\, N(y) - y^2 \frac{dN}{dy} \right]_{y=L} \qquad (5)$$

where:

k = a constant of proprtionality, and

r = the radius of a sphere of tissue in cm having the same mass stopping power as the tissue equivalent gas in the cavity

y = the lineal energy; the quotient of the mean energy imparted to the volume divided by the mean chord length in the cavity, referred to as mean event size

$N(y)$ = the event size distribution as a function of lineal energy

$\frac{dN}{dy}$ = the derivative of the event size distribution evaluated at the point where linear energy transfer and lineal energy are equal ($y=L$).

A computer code, "TEPC", performs the above calculations by evaluating the derivative using digital filter techniques to smooth the data and compute a QF.

It is not possible to distinguish between photons originating from $H(n,\gamma)D$ reactions in a phantom or tissue equivalent plastic counter and photons originating from external sources so all photon events below the lower limit (h_1) described in equation (4) are excluded in this analysis. The Rossi model also neglects energy loss effects (energy entering and leaving the counter without being detected) from very low energy neutrons, scattering, delta rays, and variation of LET along the particle track. In spite of these limitations, the Rossi model seems to be sufficiently accurate to determine QFs within one integer value, which is generally adequate for health physics purposes for neutrons with energies from 200 keV to about 10 MeV. In low energy neutron spectra such as those found inside reactor containment, the Rossi assumption encompassing low energy neutrons cannot be met. Therefore, calibration, operation, and analysis of TEPC data using the h_1 reference point actually remove a part of the low energy proton recoils and some (n,γ) events which then results in a higher QF than is expected. These errors tend

to compensate each other since photon events are excluded from the QF analysis, Rossi's method yields a high QF for neutron energies below about 200 keV where $H(n,\gamma)D$ reactions within a phantom contribute significantly to the dose and to the effective QF Brackenbush, Endres and Faust 1978).

^{3}He NEUTRON SPECTROMETER (Lucas 1979)

This section deals with the theory of operation of the ^{3}He neutron spectrometer, and its construction, calibration, and operation. Results of measurements of monoenergetic neutron beams and measurements inside PWR reactor containment are also discussed.

Theory of Operation

Neutrons interact with ^{3}He to produce a triton and a proton which are easily detected in a proportional counter. If the proton and triton are absorbed in the sensitive volume of a proportional counter, the resultant pulse height is proportional to the neutron energy plus 764 keV, the Q value of the ^{3}He(n,p)T reaction. Thermal neutrons produce events with an energy of 764 keV, which is convenient for energy calibration. The additional energy released by the reaction makes it easy to differentiate neutron induced events from gamma ray events. Unfortunately, there are competing nuclear reactions to confuse data analysis. The cross sections for these reactions as a function of neutron energy are shown in Figure 6.5. From conservation of energy and momentum it can be shown that an elastically scattered neutron [a ^{3}He(n,n') ^{3}He reaction] can deposit a maximum of 75% of its energy to the elastically scattered ^{3}He recoil. This recoil deposits 764 keV of energy if the original neutron has an energy of 1.02 MeV. Hence, neutrons with energies above 1 MeV can produce ^{3}He recoils which can be confused with events from the ^{3}He(n,p)T reaction. Above 4 Mev ^{3}He(n,d)D reactions occur which can also be confused with the ^{3}He(n,p)T reactions. Fortunately, many of these competing events can be eliminated on the basis of pulse rise time or pulse shape. The deuterons and ^{3}He recoils have linear energy transfer values higher than that of protons or tritons. Hence, for the same energy deposited in the proportional counter, the deuterons and ^{3}He recoils have

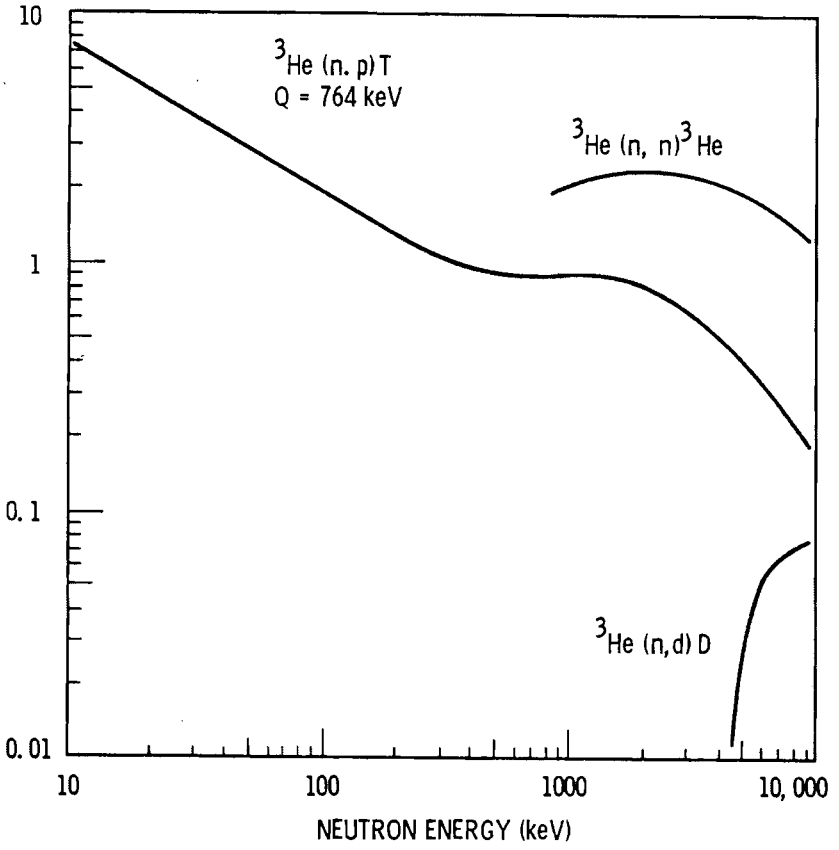

FIGURE 6.5. ^{3}He Cross Sections for Neutron Induced Charged Particle Reactions as a Function of Neutron Energy

shorter tracks. The ions produced by these shorter tracks migrate to the anode of the proportional counter in less time and produce pulses with faster risetimes. Unfortunately, if the tracks are parallel to the anode wire the pulse risetime discrimination technique does not work.

There are several properties which limit the usefulness of the ^{3}He spectrometer:

- The ^{3}He(n,p)T cross section for thermal neutrons is about 5000 barns, while that for fast neutrons is only a few barns. Thus, the detector is very sensitive to low energy neutrons and cadmium or boron absorbers and pulse pile-up circuitry must be used to prevent distortion of the measured spectrum.

- The lowest detectable energy is determined by the resolution of the proportional counter and by the peak produced by thermal neutrons, which overlaps very low energy neutron events. Some commercial ^3He proportional counters have a resolution of 2.5%, which corresponds to a full width half maximum energy of 19 keV. The practical lower energy limit for these tubes is 25 to 30 keV.

- At energies above 1.02 MeV there are competing nuclear reaction which produce pulses that can be confused with the desired $^3He(n,p)T$ reaction and complicate the proper interpretation of spectral data. Some of these competing reactions can be rejected by rise time or pulse shape analysis.

- Some neutron induced events occur near the wall or end of the counter. Charged particles striking the walls may not deposit all their energy in the sensitive volume of the proportional counter. At low neutron energies almost all of the events will deposit all their energy within the sensitive volume of the counter; a serious wall effect problem occurs at high neutron energies where the particle path lengths are about the same as the diameter of the proportional counter. To reduce wall effects, a high atom number inert gas having a greater mass stopping power, such as argon or krypton, is often added to the detector.

In spite of these apparent limitations the ^3He proportional counter spectrometer offers some real advantages:

- The ^3He detectors are very sensitive to low energy neutrons from thermal energies to 1 MeV. Few other types of spectrometers operate in this energy region.

- The data analysis of the ^3He proportional counter is straight forward and much less complicated than in other types of spectrometers.

- The components necessary to construct a ^3He spectrometer are commercially available, moderately expensive, and perhaps more rugged than those of other types of spectrometers.

- The ^{3}He spectrometer is self calibrating by using the 764 keV peak produced by thermal neutrons.
- The ^{3}He spectrometer is well suited to neutron spectrum measurements at nuclear reactors where almost all of the neutrons have energies below 1 MeV, so that competing nuclear reactions are not a problem.

Apparatus

Figure 6.6 shows a block diagram of the electronics used with the neutron spectrometer. The neutrons are detected with a one-inch diamter ^{3}He proportional counter. Signals pass through the preamp and are split into two paths. For the signal path, the pulses pass through an amplifier with 2 microsecond time constants and a pulse pile-up rejector. If two pulses occur within 12 microseconds of one another, an inhibit signal is sent to a linear gate to block the signal. Pulses are also routed along a second path through a linear amplifier with 0.5 microsecond time constants and to a pulse shape analyzer. This analyzer is adjusted to accept pulses in a narrow rise time "window," which corresponds to $^{3}He(n,p)T$ reactions. A signal is sent to a second linear gate to accept that pulse if it has the correct risetime. In the spectrometer which is used for field measurements, acceptable pulses are then routed to a multichannel analyzer. In laboratory situations the output of the pulse shape analyzer could be routed to a dual parameter analyzer to provide energy versus pulse rise time data to allow better separation of the desired $^{3}He(n,p)T$ events from competing events.

Figure 6.7 shows the importance of this electronic circuitry. To demonstrate this fact a ^{3}He proportional counter was exposed in a high dose rate field from a ^{252}Cf source. The top curve shows the results obtained without a Cd shield to eliminate thermal neutrons. At least 2 sum peaks are evident from thermal neutron events occurring almost simultaneously in the counter. The middle curve shows the effect of adding a 40-mil thick cadmium cover, which

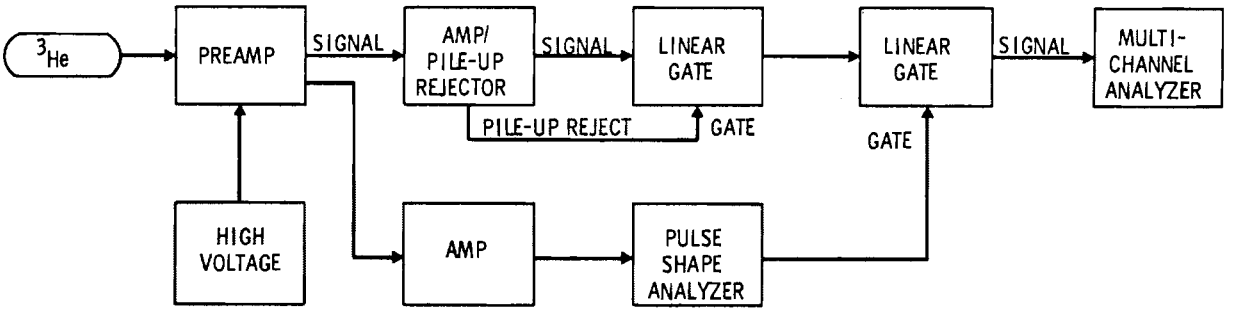

FIGURE 6.6. Block Diagram of the Electronic Equipment Used to Construct the ^{3}He Neutron Spectrometer

eliminates almost all neutrons with energies below about 0.4 eV. Some summing and pulse pile-up is still evident. The bottom curve shows the results obtained with a cadmium cover and pulse pile-up rejection and pulse shape analysis in use. Note the lack of sum peaks and virtual elimination of pulse pile-up.

The resolution and sensitivity of the ^{3}He proportional counter depends upon its physical size as well as the filling gas and fill pressure. Five to ten years ago commercially available ^{3}He proportional counters had full width half maximum (FWHM) thermal neutron peak resolutions of 8 to 15%. At the present time (1980) it is possible to purchase ^{3}He proportional counters which have resolutions of 2.3 to 3% for about $300. These improvements are due to better gas fillings and improved construction techniques. Improved resolutions can be obtained with mixtures of ^{3}He and argon gas with small amounts of carbon dioxide added. Companies making proportional counters are cleaning and outgassing the components and using center wires which are smoother, thus providing a more uniform gas gain along the length of the wire.

Neutron spectrometers used for measurements at work locations in nuclear plants must make compromises between sensitivity, or counting times and energy resolution. A 1-inch (2.5 cm) diameter tube with a 12 inch (30 cm) long active region filled with 4 psi ^{3}He, 28 psi Ar and a trace of CO_2 seems to be a reasonable compromise with reasonable sensitivity and FWHM resolution of 20 keV or better.

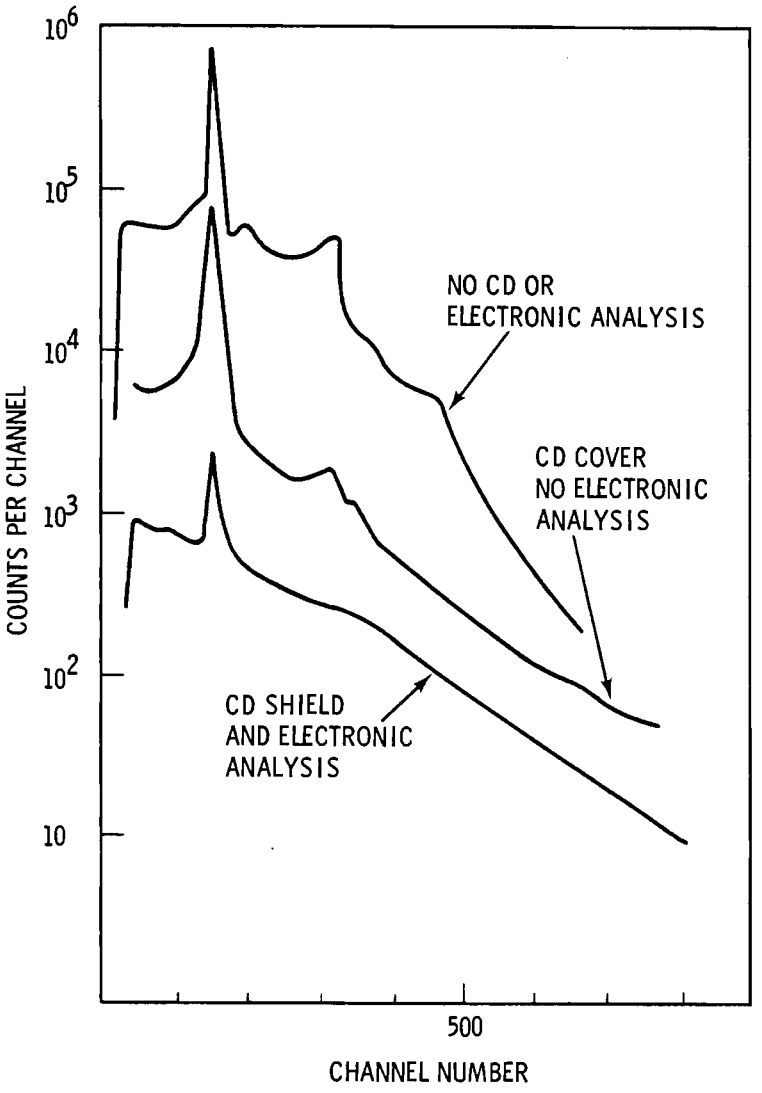

FIGURE 6.7. Effect of Cadmium Covering and Electronic Pulse Pile-Up Rejection Circuitry in Reducing the Amount of Pulse Pile-Up in High Dose Rate Neutron Fields

Calibration and Test Performance

As mentioned previously the energy calibration of the ^{3}He spectrometer is very simple. Exposing the counter to thermal neutrons produces a peak which corresponds to 764 keV. If the multichannel analyzer used to collect data is adjusted so that channel zero corresponds to zero pulse height, the keV per channel is simply 764 keV divided by the channel number of the centroid of the thermal neutron peak.

A very simple computer program called HESPEC has been written to analyze ^{3}He spectrometer data. Basically the program determines the energy calibration, i.e., the keV per channel from the thermal peak. From this information the program divides the raw data up into energy groups which have a "bin width" approximately equal to the resolution of the proportional counter used. A correction factor is then applied for the variation in cross-section with neutron energy to determine the relative neutron flux as a function of neutron energy. At the present time the program ignores wall and end effects.

The ^{3}He spectrometer system was exposed to beams of monoenergetic neutrons to check the proper operation of the system, i.e., if the experimental measurments would indeed give monoenergetic neutrons. The filtered neutron beam facility at the National Bureau of Standards was utilized for these measurements. Figure 6.8 shows the response of the spectrometer to 144 keV neutrons. A distinct peak was recorded for the 144 keV neutrons, and the small peak corresponds to 51 keV neutrons which are also present. The upper curve was obtained by correcting the data for the change in the cross section of the $^{3}He(n,p)T$ reaction with energy. The full width half maximum (FWHM) resolution of the spectrometer was determined to be about 18 keV, therefore, the next step was to expose the spectrometer to a 25 keV neutron beam to determine whether it could resolve neutrons at this lower energy. Figure 6.9 shows that indeed it is possible to resolve 25 keV neutrons under ideal conditions.

9" to 3" Sphere Ratios

One method of correcting TLD albedo dosimeter neutron response for different neutron energies involves a survey of work areas to determine an

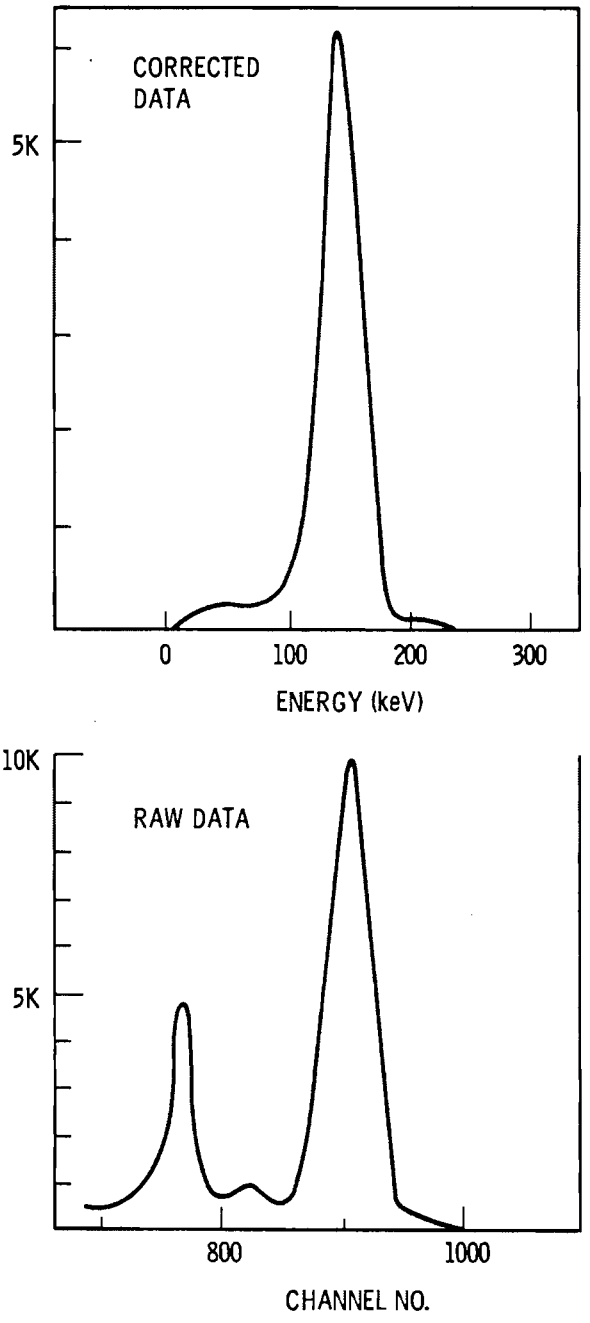

FIGURE 6.8. Results Obtained by Exposing the ^{3}He neutron Spectrometer to 144 keV Monoenergetic Neutrons at the Filtered Neutron Beam Facility at the U.S. National Bureau of Standards

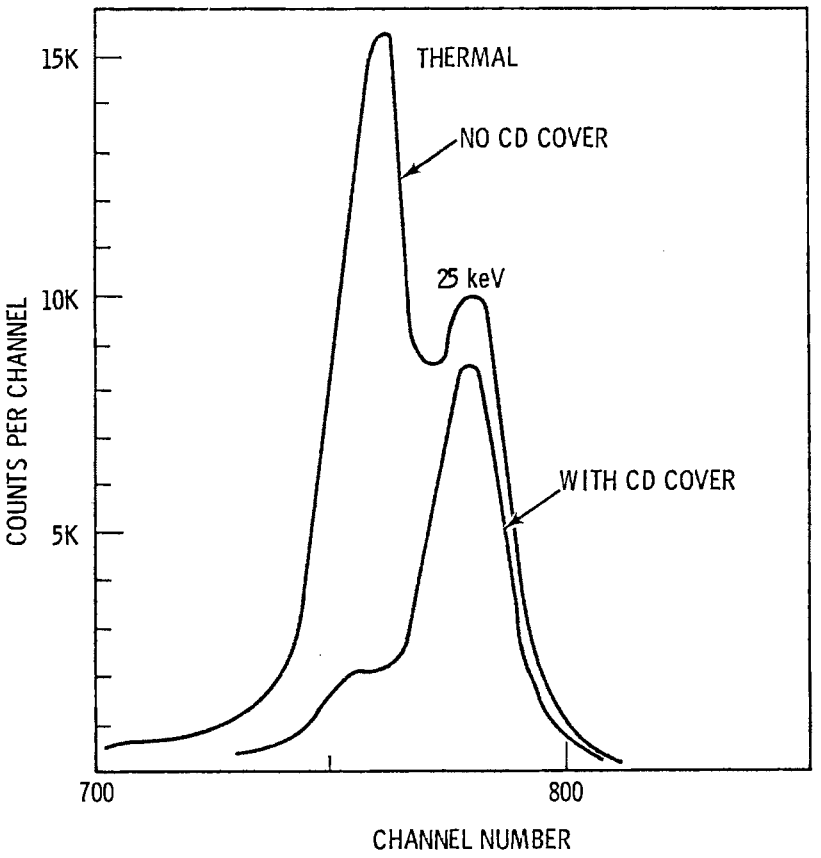

FIGURE 6.9. Results Obtained by Exposing the ^3He neutron Spectrometer to 25 keV Monoenergetic Neutrons at the Filtered Neutron Beam Facility at the U.S. National Bureau of Standards

appropriate calibration factor. The thermal neutron flux in a 23-cm-diameter (9") sphere of polyehtylene and in a 7.6-cm-diameter (3") cadmium-covered sphere of polyehtylene is determined using a BF_3 proportional counter and a commercially available survey meter. The effective TLD calibration factor can be determined from the ratio of the responses of the two spheres using Figure 6.10, which is derived from a graph presented by Griffith et al. (1979). A similar method of field measurements is reported by Reil, Scofield, and Woo (1979). This method provides correction factors which are usually accurate to within ±25%. The ratios however, can not be used to measure the average energy of the neutron spectrum because of the many uncertainties involved.

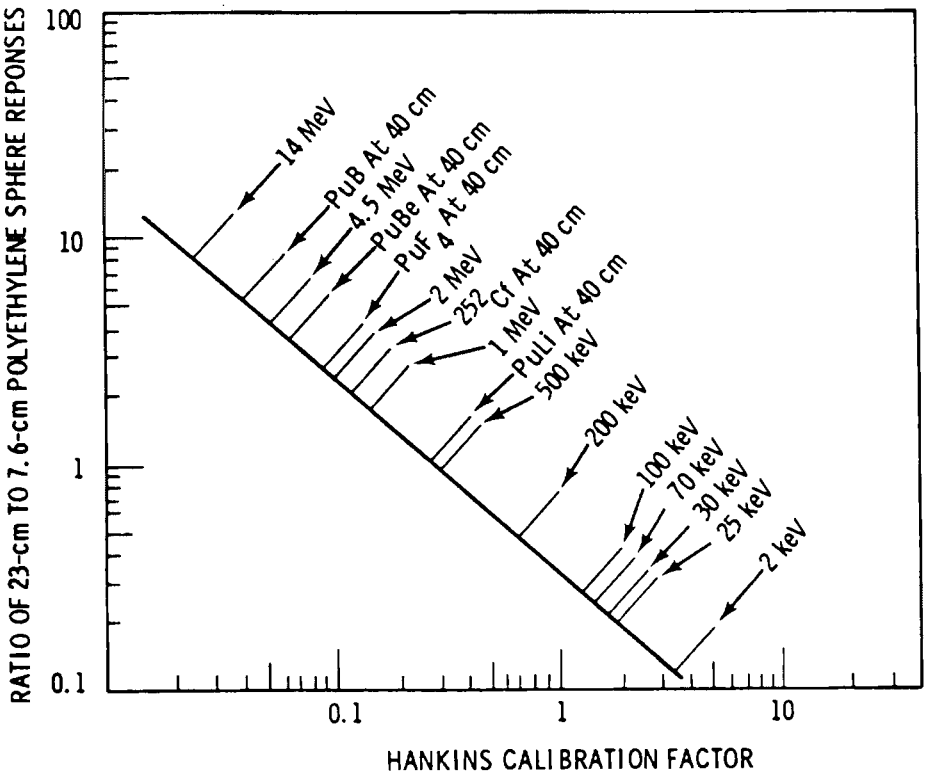

FIGURE 6.10. Effective Neutron Energy as a Function of the Ratio of 23-cm to 6.76-cm Polyethylene Sphere Responses (Griffith et al. 1979)

GAMMA SPECTROSCOPY

Field Instrument System

The major equipment used to make the gamma measurements is shown in block diagram form presented in Figure 6.11. Two types of germainium detectors were used. A 70 cc, 13% efficient lithium drifted germainium diode [Ge(Li)] having 2.20 keV full width half maximum (FWHM) resolution for the 1332 keV ^{60}Co gamma was used to take the high energy (200 keV-4 Mev) gamma measurements. A smaller intrinsic germainium (0.7 cc) with very high resolution, 202 eV FWHM at 5.9 keV and 479 eV FWHM at 122 keV (^{57}Co), was used for low energy (0-400 keV) measurements in the 308 Building. A preamplifier is connected directly to the detector output. Preamplifier power and output pulses are fed to a spectroscopy amplifier through a series of coaxial cables. The amplifier and shaped pulses are then fed to a 4096 multichannel analyzer. The spectral

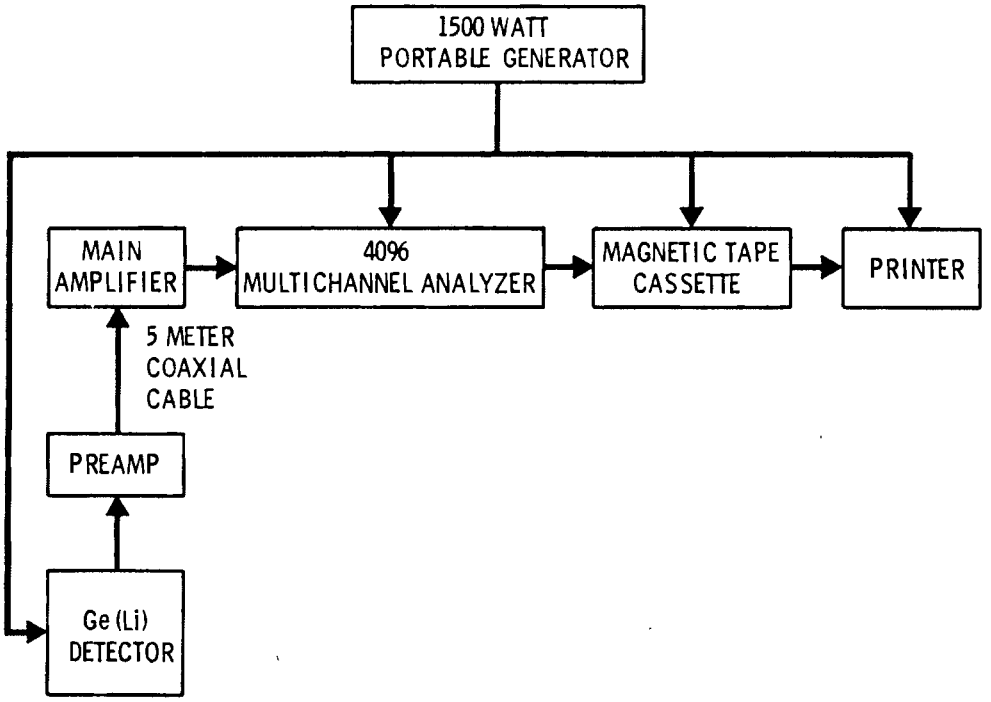

FIGURE 6.11. Simplified Layout of Equipment Used for Taking Gamma Spectrum Measurements

data are recorded on magnetic tape cassette and printed simultaneously. Power for outdoor measurements (200 West diversion box) is provided by a 1500 watt portable generator.

Data Collection and Analysis

Data analysis is done by a microprocessor based software package included in the multichannel analyzer (Canberra Model 8180, P/Q & II User's Guide). The pushbutton (hardwired) programs are used to determine energies, photopeak areas, and statistical infomration on resolved peaks. Also included is a radioisotope identification library which uses the energy of a photopeak to determine the identification of a particular radionuclide. Energy calibration is accomplished by using known radioisotope standards, such as ^{137}Cs, ^{57}Co, and ^{60}Co, whose energies and abundances are well documented (ORNL/NUREG/TM-102 1977).

Discussion

In situ field spectrometry is very useful in identifying radionuclides in the areas around diversion boxes, process lines, holding tanks, and other work areas where the actual fission and activation products need to be identified. Qualitative analysis of room/building spectra by direct counting will provide information regarding the energy spectrum at various work locations throughout the project. Figure 6.12 is typical of the data collected (actually a gamma spectrum of a hood glove in 308 Building). Results obtained for each facility are included in their respective appendix.

BETA MEASUREMENTS

A convenient field instrument for making field beta spectra measurements does not currently exist. A specially fabricated TLD dosimeter was used to obtain an estimate of beta and photon radiation penetration at the following depths:

6 mg/cm^2
30 mg/cm^2
55 mg/cm^2
89 mg/cm^2
900 mg/cm^2

Figure 6.13 shows the actual dosimeter construction and Table 6.2 indicates the filtration for each dosimeter position. Two TLD-700 chips were placed in each dosimeter card position.

Position 2 corresponds to the current "open window" filtration (89 mg/cm^2) for the Hanford dosimeter and position 3 corresponds to positions 3, 4, or 5 of the Hanford dosimeter. A beta particle of energy nearly 2 MeV is necessary to penetrate position 3. As such, position 3 is used to photon compensate the data from the other positions. To calibrate the dosimeter data, dosimeters were exposed to the uranium slab and strontium calibration sources.

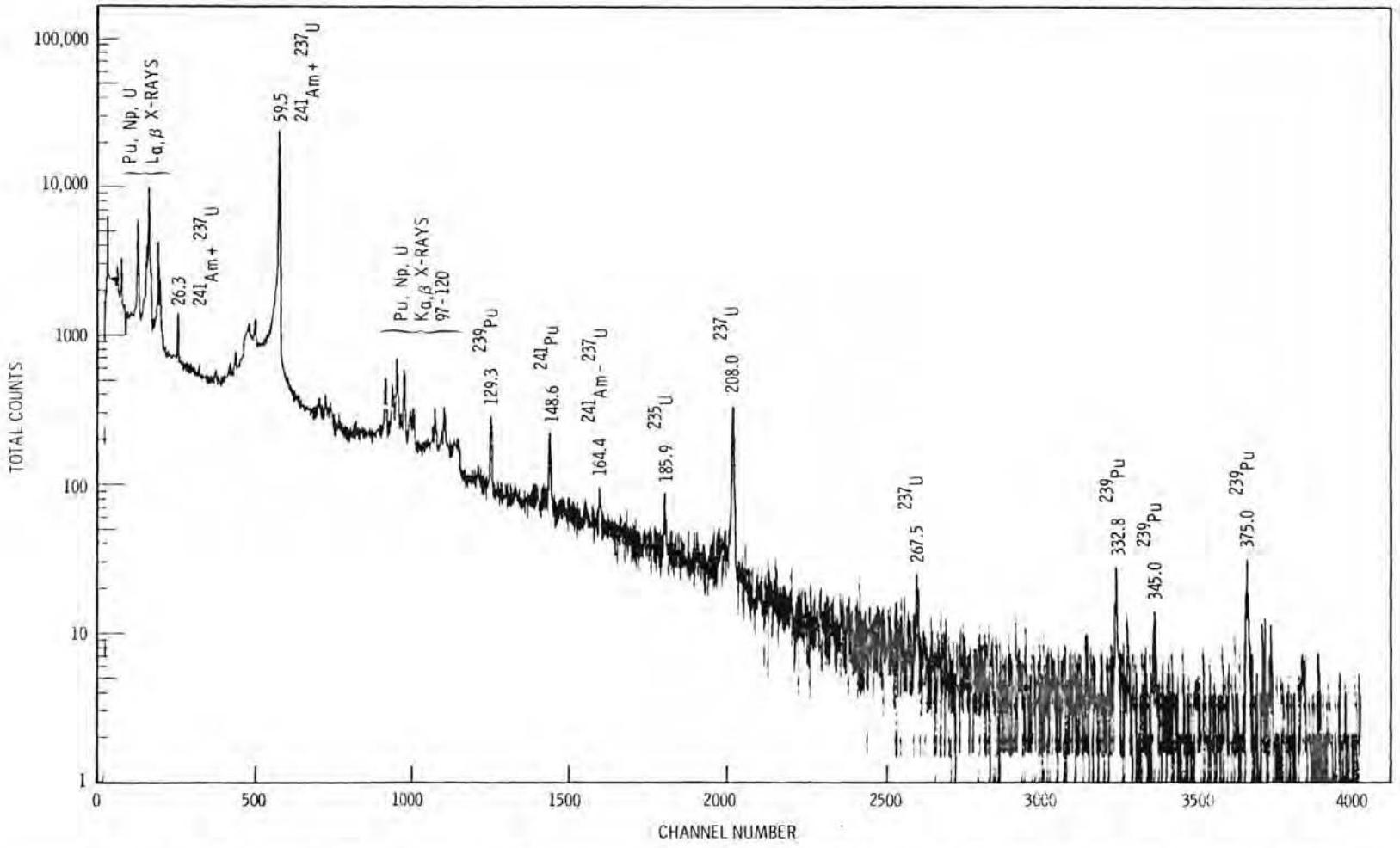

FIGURE 6.12. Photon Energy Spectrum from a Neoprene Glove Used in a Mixed Oxide (PuO_2-UO_2) Fuel Fabrication Facility

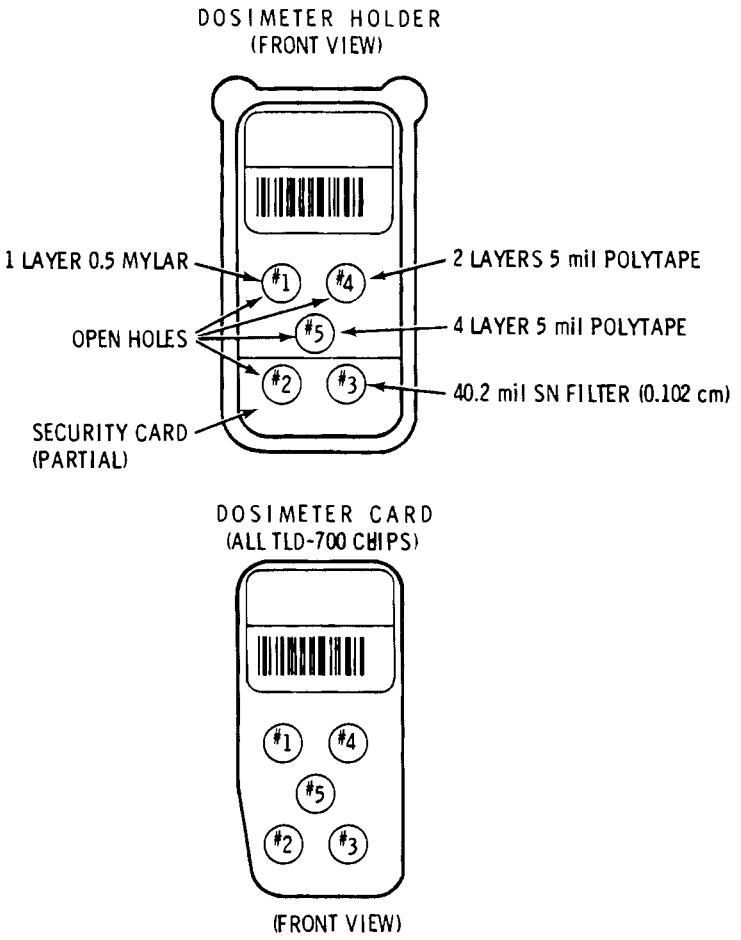

FIGURE 6.13. Modified Hanford Dosimeter for Beta Measurements

TABLE 6.2. Materials Used in Dosimeter Construction

Position Number	Dosimetry Card	Dosimeter Holder	Security Credential	Filtration	Effective Filtration
1	2 mil teflon	-		0.5 mil mylar	~6 mg/cm^2
2	2 mil teflon	-	33 mil	-	89
3	2 mil teflon	31.5 mil	33 mil	40.2 mil Sn	900
4	2 mil teflon	-	-	10 mil poly tape	30
5	2 mil teflon	-	-	20 mil poly tape	55

REFERENCES

Auxier, J. A., W. S. Snyder, and T. D. Jones. 1968. "Neutron Interactions and Penetration in Tissue." Radiation Dosimetry, Vol. 1, eds. F. H. Attix, W. C. Roesch, and E. Tochlin, (publisher, city, state).

Awschalom, M. 1966. "Use of the Multisphere Neutron Detector for Dosimetry of Mixed Radiation Fields." In: Neutron Monitoring Proceedings of a Symposium I.A.E.A.

Brackenbush, L. W., G. W. R. Endres, and L. G. Faust. (date). "Experimentally Determined Quality Factors for Fast neutrons," BNWL-SA-4249, Pacific Northwest Laboratory, Richland, Washington.

Brackenbush, L. W., G. W. R. Endres, and L. G. Faust. 1978. "Measuring Neutron Dose and Quality Factors with Tissue EQuivalent Proportional Counters." IAEA-SM-229/52, 1-11.

Bramblett, R. L., R. I. Ewing, and T. W. Bonner. 1960. "A New Type of Neutron Spectrometer. Nucl. Instruments and Methods 9:1-13.

Canberra Model 8180, P/Q a II User's Guide, Canberra Industries, Inc., 45 Gravey Avenue, Meriden, Connecticut 06450.

Glass, W. A., D. N. Samsky. 1967. "Ionization in Thin Tissue-Like Gas Layers by Monoenergetic Protons," Radiation Research 32:138-148.

Griffith, R. V. and J. C. Fisher. 1976. "Measurement of the Responses of Multisphere Detectors with Monoenergetic Neutrons, 0.1 to 18.5 MeV." Lawrence Livermore Laboratory Hazards Control Progress Report No. 51, 29-41.

Griffith, R. V., D. E. Hankins, R. B. Gammage, L. Tommasino and R. V. Wheeler. 1979. "Recent Developments in Personnel Neutron Dosimeters - A Review." Health Phys. 36:235-260.

ICRP Publication 21. 1971. "Data for protection Against Ionizing Radiation from External Sources," Supplement to ICRP Publication 15. 12, 55.

ICRU Report 20. 1976. Radiation Protection Instrumentation and Its Application. 1-8.

ICRU Report 26. 1977. Neutron Dosimetry for Biology and Medicine. 1-29

Hajnal, F. 1979. Stray Neutron Fields Inside the Containment of PWR's. IAEA-SM-242/24, International Atomic Energy Agency, Vienna, Austria.

Hankins, D. E., and R. V. Griffith. 1979. "A Survey of Neutrons Inside the Containment of a Pressurized Water Reactor." In Radiation Streaming in Power Reactors. ORNL/RSIC-43, Oak Ridge National Laboratory, Oak Ridge, Tennessee.

Lucas, A. C. 1979. "The Use of Helium-3 Filled Proportional Counter as a Sensitive Dose or Dose Equivalent Meter." IEEE Trans. Nucl. Sci. NS26:770.

Nuclear Decay Data for Radionuclides Occurring in Routine Releases from Nuclear Fuel Cycle Facilityies, ed. by D. C. Kocher, ORNL/NUREG/TM-102, Oak Ridge National Laboratory, Oak Ridge, Tennessee (August 1977).

Reil, G., N. Scofield and K. Woo. 1979. "Measurements to Determine Field Calibrations for an Albedo Neutron Dosimeter." In Abstracts of the Twenty-Fourth Annual Meeting of the Health Physics Society, Philadelphia, Pennsylvania. Health Physics Society, Denver, Colorado.

Rossi, H. H. 1968. Microscopic Energy Distribution in Irradiated Mattter. Radiation Dosimetry, Vol. 1, eds. F. H. Attix, W. C. Roesch, and E. Tochlin, (publisher, city, state).

Routti, J. T., and J. V. Sandberg. 1978. "General Purpose Unfolding Program LOUHI 78 with Linear and Non-Linear Regularization." Helsinki University of Technology, Department of Technical Physics, Report TKK-A359, 1-51.

Sanna, R. S. 1973. "Thirty One Group Response Matrices for the Multisphere Neutron Spectrometer Over the Energy Range Thermal to 400 MeV," HASL-267, 1-37.